Proceedings of the Institution of Mechanical Engineers, Part D: Journal of Automobile Engineering
http://pid.sagepub.com/

Modelling and optimization of the resistance spot welding process via a Taguchi—neural approach in the automobile industry

H-L Lin, T Chou and C-P Chou

Proceedings of the Institution of Mechanical Engineers, Part D: Journal of Automobile Engineering 2008 222: 1385
DOI: 10.1243/09544070JAUTO270

The online version of this article can be found at:
http://pid.sagepub.com/content/222/8/1385

Published by:
SAGE
http://www.sagepublications.com

On behalf of:
Institution of Mechanical Engineers

Modelling and optimization of the resistance spot welding process via a Taguchi–neural approach in the automobile industry

H-L Lin[1]*, **T Chou**[2], and **C-P Chou**[2]

[1]Department of Vehicle Engineering, Army Academy R.O.C., Jungli, Taiwan, Republic of China

[2]Department of Mechanical Engineering, National Chiao Tung University, Taiwan, Republic of China

The manuscript was received on 1 February 2006 and was accepted after revision for publication on 18 March 2008.

DOI: 10.1243/09544070JAUTO270

Abstract: Many parameters affect the quality of the resistance spot welding (RSW) process. It is not easy to obtain optimal parameters of the RSW process in the automobile industry. Conventionally, the Taguchi method has been widely used in engineering; however, with this method the desired results can only be obtained with the use of very discrete control factors, thus leading to uncertainty about the real optimum. In the process to weld the low-carbon sheet steels of the auto body, the Taguchi method was used for the initial optimization of the RSW process parameters. A neural network with the Levenberg–Marquardt back-propagation algorithm was then adopted to develop the relationships between the welding process parameters and tensile shear strength of each specimen. The optimal parameters of the RSW process were determined by simulating the process parameters using a well-trained neural network model. Experimental results illustrate the Taguchi–neural approach.

Keywords: resistance spot welding, Taguchi method, neural network

1 INTRODUCTION

Resistance welding is widely used by mass production, where production runs and consistent conditions are maintained. Resistance spot welding (RSW) is a resistance welding process that produces a weld at the facing surfaces of a joint by the heat obtained from resistance to the flow of welding current through the workpieces from electrodes that serve to concentrate the welding current and pressure at the weld area [**1**]. The RSW process is especially used in the automobile industry. Because low-carbon steel sheet has good weldability and can deform plastically to a complex shape, it is commonly used in the RSW process of an auto body. Many parameters affect the RSW quality, such as the welding current, electrode force and welding time. The desired welding parameters are usually determined on the basis of experience or handbook values. However, it does not ensure that the selected welding parameters result in optimal or near-optimal welding quality characteristics for the particular welding system and environmental conditions. Response surface methodology (RSM) is widely used to predict the weld bead geometry and mechanical properties in many welding processes. Benyounis *et al.* [**2**] developed mathematical models using RSM to predict the heat input and to describe the laser weld bead profile for the continuous-wave CO_2 laser butt welding of medium-carbon steel. The desired high-quality welds can be achieved by choosing the working condition using the developed models. However, theoretical knowledge of RSM is obscure. The calculation of RSM is relatively complicated and not easy for engineers to follow.

The Taguchi method, a popular experimental design method in industry, can overcome the shortcomings of full factorial design when carrying out fractional factorial design. The approach optimizes parameter design, but with fewer experiments. In modern quality engineering, experimental design work is performed to develop robust designs to

**Corresponding author: Department of Vehicle Engineering, Army Academy R.O.C., 113, Sec.4 Jungshan E. Rd, Taoyuan, 320, Taiwan, Republic of China. email: alaniin@ms47.hinet.net*

improve the quality of the product. Taguchi's parameter design is intended to yield robust quality by reducing the effects of environmental conditions and variations due to the deterioration of certain components [3]. However, the Taguchi method has some limitations when adopted in practice. It can find optimal solutions only within the specified level of control factors. After a parameter setting has been determined, the range of optimal solutions is set. The Taguchi method cannot find the real optimal values when the specified parameters are continuous, because it considers only the discrete control factors.

A neural network (NN) is a non-linear function, and can accurately represent a complex relationship between inputs and outputs [4–6]. A trained NN model has also been used to predict accurately the response (output) for specified parameter settings (input). Additionally, Khaw *et al.* [7] demonstrated that advantages can be gained using the Taguchi concept for NN design. First, it is the only known method for NN design that considers robustness as an important design criterion, increasing the quality of the NN. Second, the Taguchi method uses orthogonal arrays to design an NN systematically, subsequently markedly reducing the design and development time for NNs. A Taguchi–neural approach that combined the Taguchi method and an NN was used to construct a model and to determine optimal conditions for improving the quality of the RSW process. The Taguchi–neural approach consists of two phases. Phase 1 executes initial optimization via the Taguchi method to construct a database for the NN. Phase 2 applies an NN with the Levenberg–Marquardt back-propagation (LMBP) algorithm to search for the optimal parameter combination.

2 INITIAL OPTIMIZATION BY THE TAGUCHI METHOD

Low-carbon steel sheet was used in this work; its chemical composition is listed in Table 1. Plates 0.7 mm in thickness were cut into strips of size 30 mm × 100 mm. The RSW machine (FANUC α8/4000is type) was utilized for the experiment. A schematic diagram of low-carbon steel sheet specimen for RSW is shown in Fig. 1.

Table 1 Chemical composition of the material used

Material	C	Si	Mn	P	S	Fe
Amount (wt %) in MJSC270C	0.020	0.01	0.18	0.013	0.010	Balance

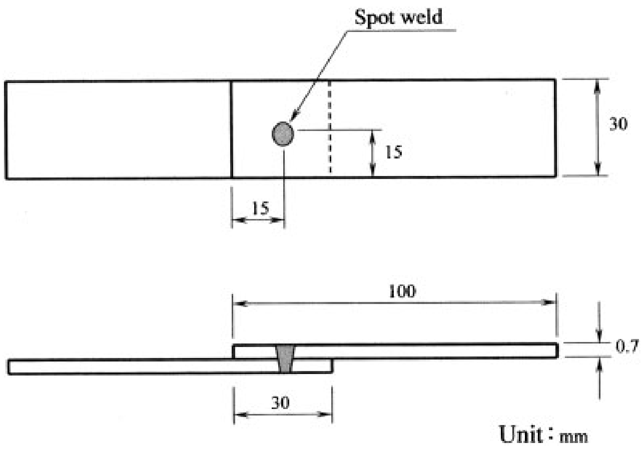

Fig. 1 Schematic diagram of the specimens

2.1 Quality characteristic of the RSW process

The study used the tensile shear strength of specimens as the quality characteristic of the process. A universal testing machine was used for this study to measure the welding tensile shear strength of the RSW specimens. The speed was set at 0.1 mm/s in the testing.

2.2 Parameters of the RSW process

Taguchi separated the factors into two main groups: control factors and noise factors. Control factors are those that allow a manufacturer to control during processing, and noise factors are expensive or difficult to control [8]. As learned from handbook and practical experience in the production of an auto body, the major welding parameters for the RSW process include the welding current, welding time, electrode force, the size of electrode tip, and the surface condition of specimens in the RSW process. The initial conditions of production operation currently are a welding current of 8000 A, a welding time of 9 cycles, an electrode force of 1.6 kN, and an electrode tip diameter of 4 mm.

By reference to the existing parameter conditions in the production line, the ranges of experimental parameter values were as follows: welding current range, 6000–12 000 A; welding time range, 6–24 cycles; electrode force range, 1.0–3.2 kN; electrode tip diameter range, 3–6 mm. The values of each welding process parameter at different levels are listed in Table 2. Moreover, the surface condition of the welding area plays a very significant role in the joint quality. It is very hard to control the surface cleanliness of the weldment in the automatic production. The cleanliness of specimens was selected as the noise factor in this study. The specimens at level 1 (designated N1), without any cleaning treatment, may

Table 2 Control factors and their levels

Factor	Process parameter	Level 1	Level 2	Level 3	Level 4
A	Electrode tip diameter	3 mm	4 mm	5 mm	6 mm
B	Welding current	6000 A	8000 A	10 000 A	12 000 A
C	Electrode force	1.0 kN	1.8 kN	2.4 kN	3.2 kN
D	Welding time	6 cycles	12 cycles	18 cycles	24 cycles

have been tarnished with dirt and/or grease. The surface impurities were removed and the surface cleaned with acetone at level 2 (specimens designated N2).

2.3 Orthogonal array experiment

Taguchi tabulated 18 basic orthogonal arrays which are called standard orthogonal arrays [**8**]. Four four-level control factors, in addition to one noise factor, were considered in this investigation. The interaction effect between the welding parameters was not considered. Therefore, there are 12 degrees of freedom owing to the four control factors. The degrees of freedom for the orthogonal array should be greater than or at least equal to those for the process parameters. The L_{16} (4^5) orthogonal array which has 15 degrees of freedom was employed in this study. An experimental layout with an inner array for control factors and an outer array for a two-level noise factor (N1 and N2) is shown in Table 3. Six repetitions (y_1, y_2, y_3, y_4, y_5, and y_6) for each trial are used with this experimental arrangement; y_1, y_2, and y_3 are N1 specimens (without cleaning); y_4, y_5, and y_6 are N2 specimens (cleaned with acetone). In the Taguchi method, repetitions are used to assess the noise effect on some quality characteristic(s) of interest. The experimental results for the tensile shear strength using the L16 orthogonal array are shown in Table 4.

2.4 Evaluation of the initial optimal condition

Taguchi created a transformation of the repetition data to another value, i.e. to a measure of the variation present. The transformation is the signal-to-noise ratio (SNR) S/N [**9**]. There are several SNRs available, depending on the type of characteristic present, such as lower is better (LB), nominal is best (NB), or higher is better (HB). The tensile-shear strength of the specimens as discussed earlier belongs to the HB quality characteristic. The SNRs, which condense the multiple data points within a trial, depend on the three-characteristic LB, NB, and HB. The equation for calculating the SNR for the HB characteristic is

$$\mathrm{SNR} = -10 \log\left(\frac{1}{n}\sum_{i=1}^{n}\frac{1}{y_i^2}\right) \qquad (1)$$

where n is the number of tests in a trial (number of repetitions regardless of noise levels). The value of n is 6 in this study. The SNRs corresponding to the tensile-shear strength value of each trial are shown in Table 4. The effect of each welding process parameter on the SNR at different levels can be separated out because the experimental design is orthogonal. Table 5 describes the SNR for each level of each control factor in the welding process. For example, the SNR for level 1 of the control factor A is computed as

$$\mathrm{SNR}_{A_1} = \frac{8.498 + 10.490 + 10.410 + 10.922}{4} = 10.080 \text{ dB}$$

Figure 2 shows the SNR graph obtained from Table 5. Basically, the larger SNR, the better is the quality characteristic (the tensile shear strength) for the specimens. The initial optimal combinations of the RSW process parameter levels, $A_1B_4C_2D_3$, can be determined from Fig. 2.

Table 3 Summary of experimental layout using an L_{16} orthogonal array

					Noise factor					
	Control factor				N1 specimens			N2 specimens		
Trial number	A	B	C	D	y_1	y_2	y_3	y_4	y_5	y_6
1	1	1	1	1	Measure data					
2	1	2	2	2						
3	1	3	3	3						
14	4	2	3	1						
15	4	3	2	4						
16	4	4	1	3						

Table 4 Summary of experimental data

Trial number	Control factors				Tensile shear strength	
	A	*B*	*C*	*D*	Average (kN)	SNR (dB)
1	1	1	1	1	2.704	8.498
2	1	2	2	2	3.366	10.490
3	1	3	3	3	3.364	10.410
4	1	4	4	4	3.584	10.922
5	2	1	2	3	2.969	9.426
6	2	2	1	4	3.244	10.181
7	2	3	4	1	3.099	9.799
8	2	4	3	2	3.036	9.617
9	3	1	3	4	2.376	7.452
10	3	2	4	3	3.340	10.470
11	3	3	1	2	3.379	10.566
12	3	4	2	1	3.526	10.922
13	4	1	4	2	1.661	4.307
14	4	2	3	1	3.199	10.064
15	4	3	2	4	3.688	11.315
16	4	4	1	3	3.783	11.554

2.5 Analysis of variance

The analysis of variance (ANOVA) is not a complicated method and has a large amount of mathematical uniqueness associated with it [**9**]. The purpose of the ANOVA is to investigate the welding process parameters that significantly affect quality. The percentage contribution to the total sum of the squared deviations can be used to evaluate the importance of a change in a welding process parameter on these quality characteristics. In addition, the *F*-test value can also be used to determine which welding process parameters have a significant effect on the quality characteristics, as shown in the equation

$$F-\text{test value} = \frac{\text{mean square due to a control factor}}{\text{mean square due to experimental error}} \quad (2)$$

Usually, when the *F*-test is less than 1, the experiment error outweighs the control factor. When the *F*-test value is approximately equal to 2, the control factor has only a moderate effect compared with the experiment error. When the *F*-test value is greater than 4, this means that a change in the process parameter has a significant effect on the quality characteristics [**10**]. When the contribution of a factor is small, as with control factor *A* (the diameter of the electrode tip) in Table 6, the sum of squares for that factor is combined with the error. This process of disregarding the contribution of a selected factor and subsequently adjusting the contributions of the other factors is known as 'pooling' [**11**]. The welding current and electrode force were the significant welding parameters that affect the quality characteristic, with the welding current being the most significant, as indicated by Table 6.

Table 5 SNR response table for the tensile shear strength

Factor	Process parameter	Level 1	Level 2	Level 3	Level 4
A	Electrode tip diameter	10.080	9.756	9.852	9.310
B	Welding current	7.421	10.301	10.523	10.754
C	Electrode force	10.200	10.538	9.386	8.875
D	Welding time	9.821	8.745	10.465	9.968

2.6 Confirmation test and proper regulation

The final step of the Taguchi method is to compare the estimated value with the confirmative experimental value, using the optimal level of the control factors to confirm the experimental reproducibility. The estimated SNR η_{opt} using the optimal level of the

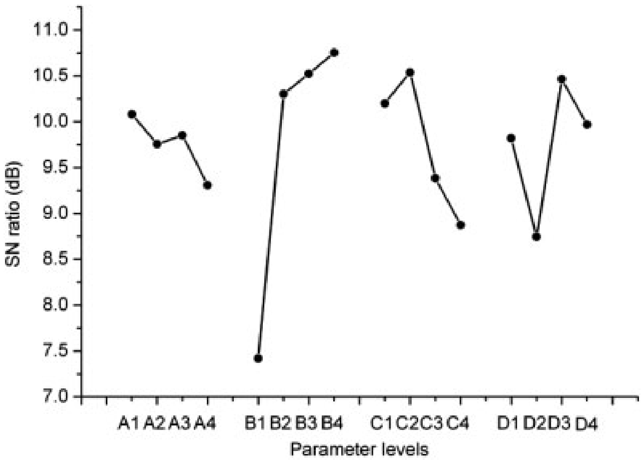

Fig. 2 SNR graph for the tensile-shear strength

Table 6 Results of ANOVA for the tensile shear strength

Factor	Process parameter	Number of degrees of freedom	Sum of squares	Mean square	F test	Pure sum of squares	Contribution (%)
A	Electrode tip diameter	3	1.253*				
B	Welding current	3	29.332	9.777	11.77	26.84	56.51
C	Electrode force	3	6.892	2.297	2.77	4.40	9.27
D	Welding time	3	6.292	2.097	2.53	3.80	8.00
Error		3	3.730				
Error (pooled)		(6)	(4.983)	(0.831)		12.46	26.23
Total		15	47.500			47.500	100

*The factor is treated as a pooled error.

control factors, can be calculated as

$$\eta_{\text{opt}} = \hat{\eta} + \sum_{j=1}^{q} \left(\eta_j - \hat{\eta} \right) \tag{3}$$

where $\hat{\eta}$ is the total average of SNR of all the experimental values, η_j is the mean SNR at the optimal level, and q is the number of control factors that significantly affect the quality characteristic.

The confidence interval (CI) is the interval between the maximum and minimum values for which the true average should fall at some stated percentage of confidence [**9**]. The confidence limits of the above estimation can be calculated taking into account the equation

$$\text{CI} = \sqrt{F_{\alpha;1;v_e} V_{\text{ep}} \left(\frac{1}{n_{\text{eff}}} + \frac{1}{r} \right)} \tag{4}$$

where $F_{\alpha;1;v_e}$ is the F ratio required for risk α, confidence equal to $1 - \text{risk}$, v_e the degrees of freedom for pooled error, V_{ep} the pooled error variance, r the sample size for the confirmation experiment, and n_{eff} the effective sample size and is given by

$$n_{\text{eff}} = \frac{N}{1 + \text{DOF}_{\text{opt}}} \tag{5}$$

where N is the total number of trials and DOF_{opt} is the total degrees of freedom associated with items used in the η_{opt} estimate. With a confidence of 95 per cent for the tensile shear strength, $F_{0.05;1;6} = 5.99$, and $V_{\text{ep}} = 0.831$ (from Table 6), the sample size r for the confirmation experiment is 2, $N = 16$, $\text{DOF}_{\text{opt}} = 9$, and the effective sample size is $n_{\text{eff}} = 1.6$. Thus, the CI is computed to be 2.37 dB. The experimental results (Table 7) confirm that the initial optimizations of the RSW process parameters were achieved.

Although the conformity of reproducibility for the experimental results has been confirmed with an average tensile shear strength of the specimens as high as 3.812 kN, however, a spark phenomenon took place between the specimens and the electrode during the spot welding process, which leads to a severely shortened life cycle of the electrode and a collaterally affected joint quality of weldment for subsequent welding. With the ANOVA outcomes (Table 6) referenced, a proper regulation of the welding current is necessary to cope with the above-mentioned defects. As can be seen from Fig. 2 (the SNR graph), the SNR was slightly increased when the welding current increased from 8000 A to 12 000 A, i.e. the tensile shear strength of specimens was not increased greatly. Therefore, the optimal conditions of parameters obtained from application of the Taguchi method remained unchanged except that the welding current was changed from 12 000 A to 8000 A. Table 8 lists the experimental results after the parameters had been adjusted.

3 NEURAL NETWORK

NNs are used for the modelling of complex manufacturing processes, usually with regard to process

Table 7 Results of the confirmation experiment

Trial number	Tensile shear strength								Confidence interval (95%)
	N1 specimens			N2 specimens			SNR (dB)	Average (kN)	
17	4.062	3.955	3.945	3.745	3.622	3.579	11.607	3.812	12.257 ± 2.37 (dB)
18	3.995	3.672	3.857	3.707	3.701	3.9043	11.597		

Table 8 Results of the Taguchi method with proper regulation

Trial number	Tensile shear strength						Average (kN)
	N1 specimens			N2 specimens			
19	3.485	3.297	3.294	3.605	3.431	3.221	3.375
20	3.334	3.172	3.368	3.583	3.411	3.296	

and quality control [**12**, **13**]. Several well-known supervised learning networks use a back-propagation (BP) NN. Funahashi [**14**] proved that a BP NN may approximately realize any continuous mapping. BP learning employs a gradient-descent algorithm to minimize the mean-square error (MSE) between the target data and the predictions of an NN. However, one of the major problems with the conventional BP algorithm (the gradient-descent algorithm) is the extended training time required. The techniques for accelerating convergence have fallen into two main categories: heuristic methods and standard numerical optimization methods such as the LMBP algorithm [**15**].

3.1 The Levenberg–Marquardt back-propagation algorithm

The LMBP algorithm is similar to the quasi-Newton method, in which a simplified form of the Hessian matrix (second derivatives) is used. When the cost function has the form of a sum of squares, then the Hessian matrix **H** can be approximated as

$$\mathbf{H}=\mathbf{J}^{\mathrm{T}}\mathbf{J} \tag{6}$$

and the gradient can be computed as

$$\boldsymbol{g}=\mathbf{J}^{\mathrm{T}}\boldsymbol{e} \tag{7}$$

where **J** is the Jacobian matrix that contains the first derivatives of the network errors with respect to the weights and biases and $\boldsymbol{e}$ is a vector of network errors. The Jacobian matrix can be computed through a standard BP technique that is much less complex than computing the Hessian matrix [**16**].

An iteration of this algorithm can be written as

$$\boldsymbol{X}_{K+1}=\boldsymbol{X}_{K}-\left(\mathbf{J}^{\mathrm{T}}\mathbf{J}+\mu\mathbf{I}\right)^{-1}\mathbf{J}^{\mathrm{T}}\boldsymbol{e} \tag{8}$$

When the scalar μ is zero, this is just Gauss–Newton behaviour using the approximate Hessian matrix. When μ is large, this becomes gradient-descent type with a small step size.

3.2 The parameters of the LMBP algorithm

The algorithm begins with μ set to some small value. If a step does not yield a smaller value for $\boldsymbol{e}$, then the step is repeated with μ multiplied by some factor $\theta>1$. Eventually $\boldsymbol{e}$ should be decreased since a small step in the direction of steepest descent would be taken. If a step does produce a smaller value for $\boldsymbol{e}$, then μ is divided by θ for the next step, ensuring that the algorithm will approach Gauss–Newton behaviour, which should provide faster convergence [**15**]. The LMBP algorithm is the fastest algorithm that has been tested for training multilayer networks of moderate size, even though it requires a matrix inversion at each iteration. It requires two parameters, but the algorithm does not appear to be sensitive to this selection.

4 APPLICATION OF THE BP NEURAL NETWORK

4.1 Training of the BP network

An NN, which can capture and represent the relationship between the process variables and process outputs, was developed in this stage. Multilayer perceptions are feedforward NNs commonly used to solve difficult predictive modelling problems [**17**]. They usually consist of an input layer, one or more hidden layers, and one output layer. The neurons in the hidden layers are computational units that perform non-linear mapping between inputs and outputs. A feedforward NN was adopted in this study. It takes a set of five input values (the control factors A, B, C, and D and a noise factor) and predicts the value of one output (the tensile-shear strength of the specimen). The transfer functions for all hidden neurons are tangent sigmoid functions, as shown in the equation

$$f(x)=\frac{\exp(x)-\exp(-x)}{\exp(x)+\exp(-x)} \tag{9}$$

The transfer functions for the output neurons are linear functions [**18**].

Determining the number of hidden neurons is critical to the design of NNs. An over-abundance of hidden neurons provides too much flexibility, which usually causes overfitting. However, too few hidden neurons restrict the learning capability of a network and degrade its approximation performance [**17**]. A total of 96 input–output data patterns were separated into a training set, a testing set, and a validating set. Functionally, 60 per cent (58 patterns) were randomly selected for training the NN, 20 per cent (19 patterns) were randomly selected for testing, and 20 per cent (19 patterns) were randomly selected for validating. An efficient algorithm, namely the Levenberg–Marquardt algorithm, was used to improve classical BP learning in the training process [**15**, **17**]. The NN software MATLAB Neural Network ToolBox was used to develop the required network. The performance of each NN was measured with the MSE of the testing subset. It must be noted that, because the outcome of the training greatly depends on the initialization of the weights, this is done randomly according to the Nguyen–Widrow technique [**19**]. Therefore, each NN was trained three times and the average MSE was calculated. The results for seven networks tested are presented in Table 9. They show that the best performing NN was the 5–4–1 which displayed an average MSE of 5.78 per cent together with a minimum MSE that was equal to 3.15 per cent. The topology of the 5–4–1 network with a μ value of 0.001 and a θ value of 10 is depicted in Fig. 3.

4.2 Simulation with a well-trained network

The control factor A (the diameter of the electrode tip) is an insignificant welding parameter that affects the quality characteristic, as shown in Table 6. First, the trained network 5–4–1 with 3.15 per cent MSE value was employed as the simulating function of the control factor A. Figure 4 compares results simulated using the control factor A, the other conditions ($B = 8000$ A, $C = 1.8$ kN, and $D = 18$ cycles) indicating that the tensile shear strength of specimens is optimal for setting the diameter of the electrode tip to 6 mm. Second, Fig. 5 compares results simulated using the control factor D, the other conditions ($A = 6$ mm, $B = 8000$ A, and $C = 1.8$ kN) indicating that the tensile shear strength of specimens is optimal for setting the welding time to 15 cycles. Third, Fig. 6 compares results simulated using the control factor C, the other conditions ($A = 6$ mm, $B = 8000$ A, and $D = 15$ cycles) indicating that the tensile shear strength of specimens is optimal for setting the electrode force to 1.9 kN. Finally, Fig. 7 compares results simulated using the control factor D, the other conditions ($A = 6$ mm, $C = 1.9$ kN, and $D = 15$ cycles) indicating that a welding current over 9000 A may be more sensitive for the cleanliness of specimens. In addition, it can be seen that the welding current and tensile shear strength are in direct ratio until about 9000 A. The welding current of the RSW process for the initial condition is 8000 A. Therefore, a welding current of 8000 A has been selected in this study.

Table 9 Options for different networks

Architecture (input–hidden unit–output)	MSE for training			
	Train 1	Train 2	Train 3	Average
5–2–1	0.2997	0.1208	0.2480	0.2228
5–3–1	0.2174	0.1923	0.0653	0.1583
5–4–1	**0.0587**	**0.0315**	**0.0833**	**0.0578**
5–5–1	0.0548	0.0948	0.1258	0.0918
5–6–1	0.0435	0.0413	0.1518	0.0789
5–7–1	0.1242	0.1196	0.0489	0.0976
5–8–1	0.0703	0.1017	0.0330	0.0683

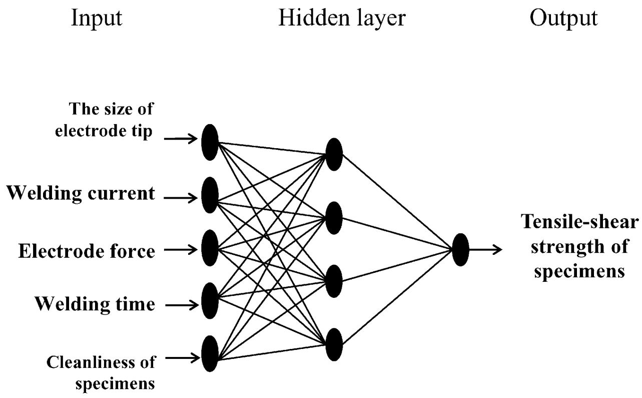

Fig. 3 The BP network topology

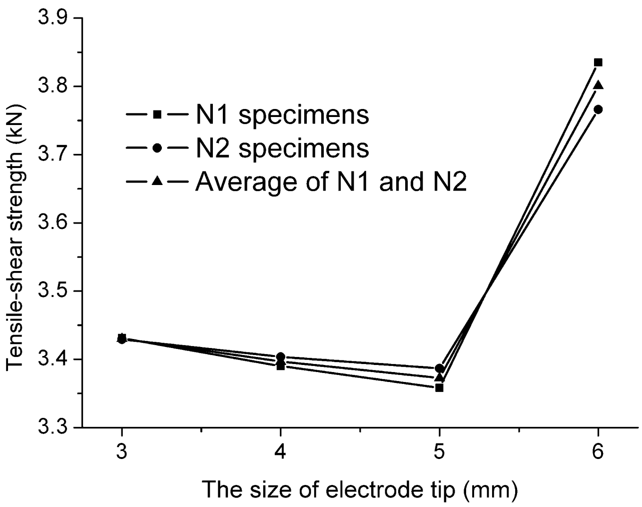

Fig. 4 Results of simulating different sizes of the electrode tip

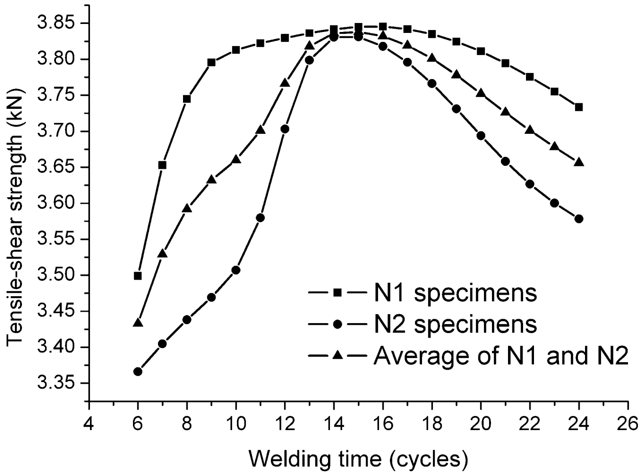

Fig. 5 Results of simulating different welding times

4.3 Comparison of the experimental results

Combining the Taguchi method and NNs yielded a welding condition that optimized the tensile shear strength of an RSW specimen: electrode tip diameter, 6 mm; welding current, 8000 A; electrode force, 1.9 kN; welding time, 15 cycles. Table 10 presents the experimental results obtained using these optimal welding parameters. Table 11 presents the experimental results obtained using the present conditions of production operation currently ($A = 4$ mm, $B = 8000$ A, $C = 1.6$ kN, and $D = 9$ cycles). Comparing Table 8 with Table 11 reveals that the increase in average tensile shear strength from the initial condition to the initial optimal parameters (apply the Taguchi method only) is 0.133 kN. Comparing Table 10 with Table 11 reveals that the increase in average tensile shear strength from the initial condition to the real optimal parameters (apply the Taguchi–neural approach) is 0.409 kN. In summary, the quality of the RSW process for low-carbon steel sheet can be efficiently improved through the Taguchi–neural approach.

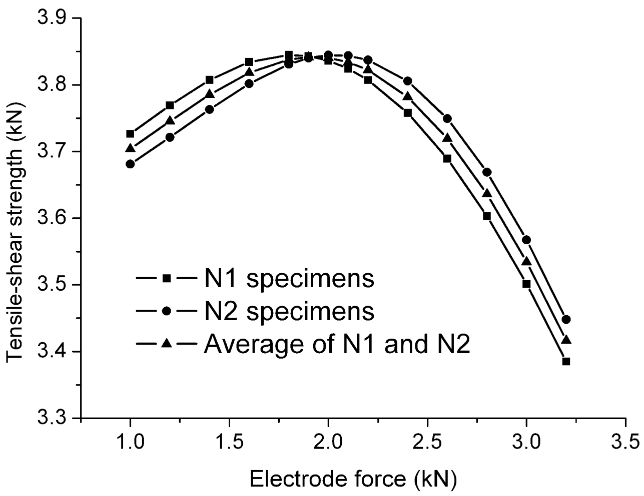

Fig. 6 Results of simulating different electrode forces

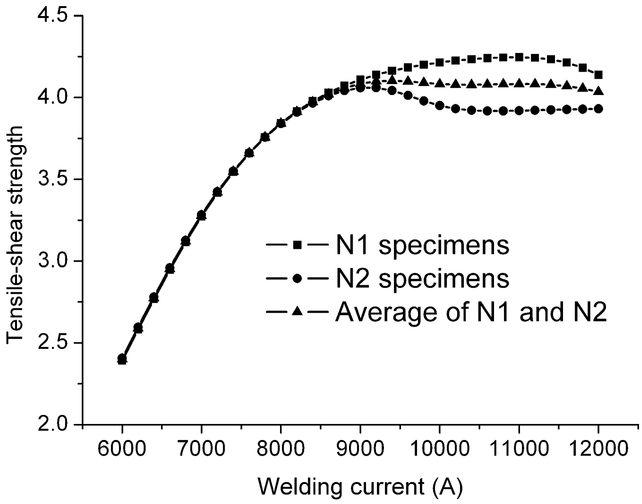

Fig. 7 Results of simulating different welding currents

5 CONCLUSIONS

1. The improvement in the average tensile shear strength from the initial conditions to the initial optimal parameters (apply the Taguchi method only) is about 4.1 per cent. The improvement in the average tensile shear strength from initial conditions to the real optimal parameters (apply the Taguchi–neural approach) is about 12.6 per cent.
2. The NN with the LMBP algorithm represents an easy and quick method to explore a non-linear model. The well-trained model may help engineers to predict precisely the tensile shear strength of specimens and to adjust welding parameters effectively for the RSW process in the future.
3. The Taguchi–neural approach allows engineers to use neural network software directly to optimize the parameters of the RSW process without any theoretical knowledge of neural computing.

Table 10 Results of the Taguchi–neural approach

Trial number	Tensile shear strength						Average (kN)
	N1 specimens			N2 specimens			
21	3.652	3.787	3.780	3.424	3.612	3.596	3.651
22	3.589	3.572	3.686	3.851	3.684	3.579	

Table 11 Results of the initial conditions

Trial number	Tensile shear strength						Average (kN)
	N1 specimens			N2 specimens			
23	3.136	3.317	3.214	3.285	3.294	3.357	3.242
24	3.199	3.115	3.207	3.373	3.223	3.179	

ACKNOWLEDGEMENT

The authors acknowledge Mr Gao Liang-Wei, Engineer of the Production Engineering Division of China Motor Co., Ltd, Taiwan, for permitting the use of the RSW machine in this study.

REFERENCES

1 **Cary, H. B.** *Modern welding technology*, 1994 (Prentice-Hall, Englewood Cliffs, New Jersey).
2 **Benyounis, K. Y., Olabi, A. G.,** and **Hashmi, M. S. J.** Effect of laser welding parameters on the heat input and weld-bead profile. *J. Mater. Processing Technol.*, 2005, **164–165**, 978–985.
3 **Taguchi, G., Elsayed, E. A.,** and **Hsiang, T. C.** *Quality engineering in production systems*, 1989 (McGraw-Hill, New York).
4 **Su, C. T., Chiu, C. C.,** and **Chang, H. H.** Parameter design optimization via neural network and genetic algorithm. *Int. J. Ind. Engng*, 2000, **7**(3), 224–231.
5 **Kim, I. S., Jeong, Y. J.,** and **Lee, C. W.** Prediction of welding parameters for pipeline welding using an intelligent system. *Int. J. Advd Mfg Technol.*, 2003, **22**, 713–719.
6 **Bhadeshia, H. K. D. H., Mackay, D. J. C.,** and **Svensson, L. E.** Impact toughness of C–Mn steel arc welds – Bayesian neural network analysis. *Mater. Sci. Technol.*, 1995, **11**, 1046–1051.
7 **Khaw, J. F. C., Lim, B. S.,** and **Lim, L. E. N.** Optimal design of neural networks using Taguchi method. *Neurocomputing*, 1995, **7**, 225–245.
8 **Phadke, M. S.** *Quality engineering using robust design*, 1989 (Prentice-Hall, Englewood Cliffs, New Jersey).
9 **Ross, P. J.** *Taguchi techniques for quality engineering*, 1988 (McGraw-Hill, New York).
10 **Fowlkes, W. Y.** and **Creveling, C. M.** *Engineering methods for robust product design*, 1995 (Addison-Wesley, Reading, Massachusetts).
11 **Roy, R. K.** *A primer on the Taguchi method*, 1990 (Van Nostrand Reinhold, New York).
12 **Su, C. T.** and **Chiang, T. L.** Optimizing the IC wire bonding process using a neural networks/genetic algorithms approach. *J. Intell. Mfg*, 2003, **14**, 229–238.
13 **Coit, D. W., Jacson, B. T.,** and **Smith, A. E.** Static neural network process model: considerations and case studies. *Int. J. Prod. Res.*, 1998, **36**(11), 2953–2967.
14 **Funahashi, K.** On the approximate realization of continuous mapping by neural network. *Neural Networks*, 1989, **2**, 183–192.
15 **Hagan, M. T., Demuth, H.,** and **Beale, M.** *Neural network design*, 1996 (PWS Publishing Company, Boston, Massachusetts).
16 **Hagan, M. T.** and **Menhaj, M. B.** Training feedforward networks with the Marquardt algorithm. *IEEE Trans. Neural Networks*, 1994, **5**(6), 989–993.
17 **Haykin, S.** *Neural networks – a comprehensive foundation*, 1994 (Macmillan, London).
18 **Demuth, H.** and **Beale, M.** *Neural network toolbox – for use with MATLAB*, 1998 (The Mathworks, Inc., Natick, Massachusetts).
19 **Benardos, P. G.** and **Vosniakos, G. C.** Prediction of surface roughness in CNC face milling using neural networks and Taguchi's design of experiments. *Robotics Computer Integrated Mfg*, 2002, **18**, 343–354.